

FRACTURE-MECHANICS CHARACTERISTICS OF M-2-TYPE HIGH-SPEED STEEL

LOMNO-MEHANSKE ZNAČILNOSTI HITROREZNEGA JEKLA VRSTE M-2

Guy Pluvina¹, Borivoj Šuštaršič², F. Montannari¹, Joseph Gilgert¹,
Vojteh Leskovšek², Jelena Vojvodič Tuma²

¹ Reliability Mechanics Laboratory, University of Metz, Ile du Saulcy, Metz, France

² Institute of Metals and Technology, Lepi pot 11, 1000 Ljubljana, Slovenia
pluvina@sciences.univ-metz.fr

Prejem rokopisa – received: 2003-10-01; sprejem za objavo – accepted for publication: 2004-04-13

This study presents some of the investigations made in the frame of the project called *Determination of notch fracture toughness of tool steels*, which is part of the Slovenia-France bilateral scientific cooperation named Proteus. The paper presents a determination of the notch fracture toughness with a non-standardised method. This is the so-called determination of the notch stress-intensity factor $K_{\rho,c}$ on specimens without a fatigue crack but with different notch radii. For the investigations and experiments, hard and brittle, M-2-type high-speed steel was selected. During loading it behaves in a completely linear-elastic way to the point of fracture. In the introduction, the volumetric approach is presented, where it is assumed that material fracture starts and continues if an appropriately large physical volume is available and that this volume is loaded with a certain average equilibrium stress. The basis for the determination of the effective volume, the distance and the stress is a numerical calculation based on the finite-element method (FEM). The results of the FEM calculations are presented and discussed. The experimental procedures and the results of the method are also presented. The experimental results are supported by microstructural and fractographic examinations.

Key words: HSS steel, fracture toughness, critical notch stress-intensity factor

V prispevku predstavljamo del raziskav, ki je bil opravljen v okviru projekta z naslovom: Določevanje lomne žilavosti orodnih jekel na preizkušancih z zarezo, pod okriljem Slo-F bilateralnega znanstvenega sodelovanja Proteus. Prikazan je nestandardni način določevanja faktorja intenzitete napetosti v zarezi $K_{\rho,c}$ brez utrujenostne razpoke toda z različnimi korenskimi polmeri. Za preiskave smo izbrali trdo in krhko hitrorezno jeklo vrste M-2, ki se vede linearno-elastično praktično do loma. Predstavljen je volumetrični lomno-mehanski način, kjer je privzeto, da se proces loma prične in nadaljuje, če je za to na razpolago neki ustrezen velik fizikalni volumen, na katerega deluje neka povprečna uravnotežena napetost. Določevanje efektivne prostornine, razdalje in napetosti temelji na numeričnih izračunih z metodo končnih elementov. Predstavljamo potek in rezultate računalniške simulacije na osnovi metode končnih elementov za določitev efektivne napetosti in efektivne razdalje v korenu zareze, ki so osnova za določitev kritičnega faktorja intenzitete napetosti v zarezi. V nadaljevanju podajamo potek preizkusov in eksperimentalne rezultate določevanja lomne žilavosti v zarezi, ki so podprti z mikrostrukturnimi in fraktografskimi preiskavami.

Ključne besede: hitrorezno jeklo, lomna žilavost, kritični faktor zarezne intenzitete napetosti

1 INTRODUCTION

Some materials, for example, ferritic steels, exhibit a brittle-to-ductile transition. This transition is promoted by an increased temperature or a decreased loading rate. Such an effect can be explained by the fact that much more plasticity is necessary to initiate a ductile than a brittle fracture process, and plasticity is a thermally activated process. However, a third physical parameter influences this transition, i.e., the notch radius, as controlled via the level of stress triaxiality. Some experimental observations of $K_{\rho,c}$ versus $\sqrt{\rho}$, and for a critical notch radius ρ_c , have revealed that $K_{\rho,c}$ is independent of ρ . Similarly, the presence of a ductile plateau is independent of the notch radius. In the transition regime, $K_{\rho,c}$ is a linear function of the square root of the notch radius, and a similar transition curve can be drawn which represents, more generally, the notch effect on the stress-intensity factor. Such behaviour was observed by several authors^{1,2}. In order to

take into account any notch geometry, the critical notch stress-intensity factor is plotted versus ρ^α . The exponent α is a stress-distribution parameter, which characterises the pseudo-stress singularity at the notch tip, and the notch sensitivity m can be represented by the slope β of the transition line³:

$$m = \tan g(\beta) \quad (1)$$

The shape of the transition curve is sensitive to yield stress. The critical notch-root radius decreases with a decrease in the yield stress. Generally speaking, the larger critical notch radii are detected for high-strength steels, i.e., steels with high notch sensitivity, rather than tough steels with lower yield stresses. Also, when increasing the yield stress the notch sensitivity is strongly reduced and the ductile plateau disappears.

The main problem with using pre-cracked specimens to determine fracture toughness is the costly and time-consuming process of pre-cracking. This is an important point when there is a need to make several

identical tests to obtain a statistical analysis. This is the reason why we decided to look at the possibility of using *Notch Fracture mechanics* and notched specimens to determine the fracture toughness on the selected steel, where the conditions are more difficult because of the absence of the brittle plateau.

2 MATERIAL AND SPECIMENS

The investigated high-alloyed high-speed steel (HSS) was produced by a standard casting procedure (melting in an electro-arc furnace, ingot casting, hot forging and rolling). This type of steel has a characteristic non-homogeneous distribution of primary carbides in the steel matrix (**Figure 1a**). The chemical composition of the steel is given in **Table 1**.

Table 1: Nominal and actual chemical composition of the selected M-2-type HSS

Tabela 1: Nominalna in dejanska kemična sestava izbranega hitroreznega jekla vrste M-2

Alloy composition	Chemical composition – the mass fractions (%)					
	C	Cr	W	Mo	V	Co
Nominal	0.85	4.0	6.0	5.0	2.0	-
Actual	0.88	3.88	6.16	4.84	1.82	

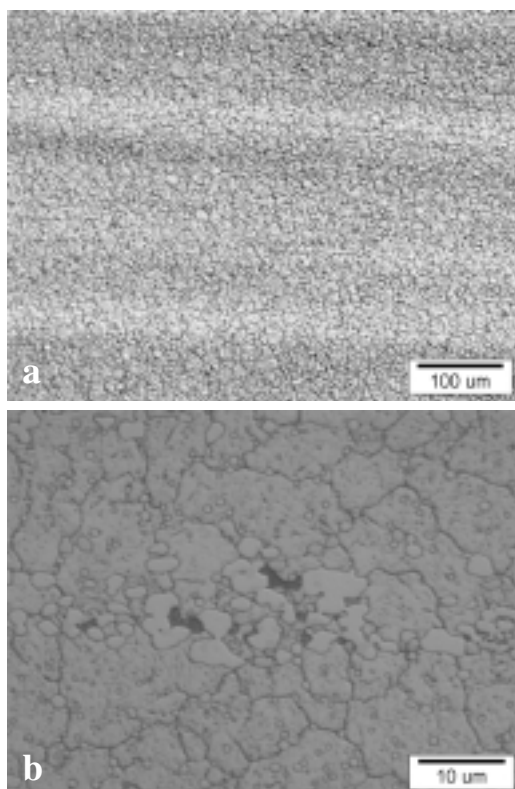


Figure 1: Microstructure of selected HSS in optical microscope: **a)** carbide stringers (magnification x100) and **b)** carbide clusters (magnification x1000), etched (nital)

Slika 1: Mikrostruktura izbranega hitroreznega jekla pod optičnim mikroskopom: **a)** karbidna trakavost (originalna povečava 100-krat in **b)** karbidni skupki (povečava 1000-krat), jedkano v nitalu

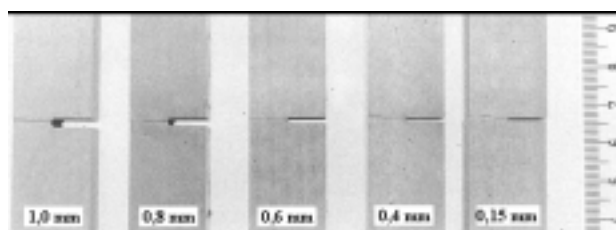


Figure 2: Fractured SENB samples with different notch radii

Slika 2: Prelomljeni preizkušanci SENB z različnim polmerom U-zareze

In addition to this basic chemical composition, the following elements are also present: 0.005 % S, 0.025 % P, 0.21 % Si, 0.26 % Mn, 0.1 % Ni, 0.008 % Al, 0.13 % Cu and 0.017 % Sn.

The vacuum heat-treatment conditions are as follows: austenitising at 1180 °C, fast cooling under nitrogen pressure (5 bars) to 80 °C and then two times tempering at 500 °C for one hour. The steel microstructure consists of a steel matrix (tempered martensite), a dispersion of relatively rough primary carbide particles, sometimes in clusters (**Figure 1 b**), and of some retained austenite. This material is linearly elastic until fracture. The basic mechanical properties of this type of steel are: $E = 210$ GPa, $\nu = 0.3$ and $R_m = 1700$ MPa. For our investigations, SENB (Single Edge Notched Bend) specimens with U notches of different notch radii: $\rho = (0.15, 0.4, 0.6, 0.8$ and $1.0)$ mm; (**Figure 2**) made by electro erosion were used. The basic dimensions of the samples are: length $L = 120$ mm, thickness $B = 20$ mm, width $W = 20$ mm and notch length $a = 10$ mm.

3 EXPERIMENTAL RESULTS

The specimens were loaded in bend mode until failure. Three tests were performed for each specimen geometry. The behaviour is purely linear elastic with a very low scatter. Three quasi-identical load-displacement curves for the same specimen geometry were obtained and the critical load was defined in this case with the maximum load. The results in terms of critical load are listed in **Table 2**.

Table 2: Critical load and critical displacement for each fracture test

Tabela 2: Kritična obremenitev in kritičen pomik za preizkušance z različno zarezo

ρ /mm	0.15	0.40	0.60	0.80	1.00
F_{max} /kN	15.40	18.50	21.3	23.76	24.233
δ /mm	0.165	0.223	0.257	0.292	0.297

In the plot of the mean values of the fracture load versus the notch radius, the fracture load increases linearly with the notch radius up to $\rho = 0.8$ mm, and then less rapidly after this value (**Figure 3**). **Figure 4** shows an SEM micrograph of a typical fracture surface of SENB samples at the crack-initiation site.

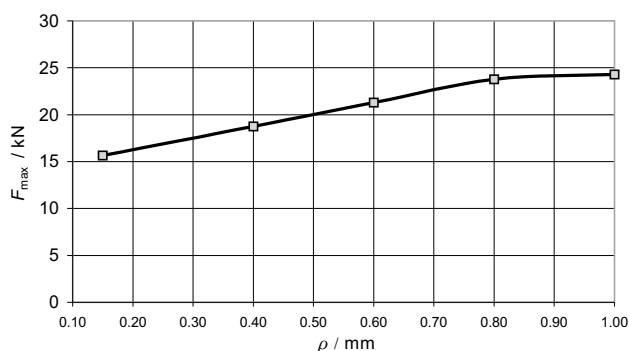


Figure 3: Plot of the mean value of the fracture load F_{max} versus the notch radius ρ of the SENB specimens

Slika 3: Odvisnost med maksimalno upogibno silo F_{max} , potrebno za porušitev preizkušancev, in njihovim polmerom zarez ρ

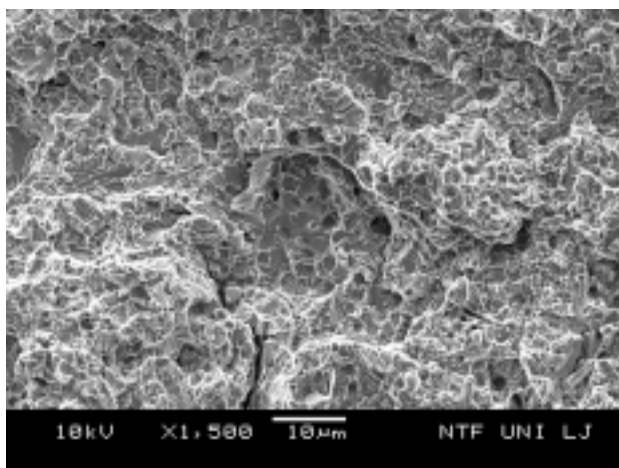


Figure 4: Fracture surface of an SENB specimen with a notch radius $\rho = 1.0$ mm at the crack-initiation site (SEM, original magnification $\times 1500$)

Slika 4: Prelomna površina SENB preizkušanca s polmerom zarez $\rho = 1,0$ mm na mestu iniciacije razpoke (SEM, originalna povečava 1500-krat)

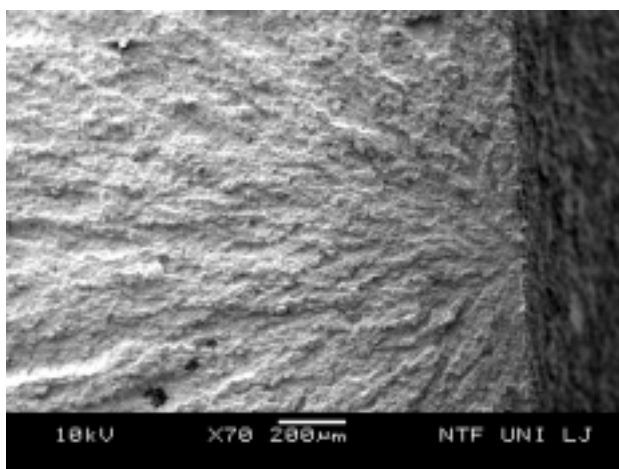


Figure 5: Fracture surface of an SENB sample with a notch radius $\rho = 1.0$ mm at the crack-initiation site (SEM, original magnification $\times 70$)

Slika 5: Prelomna površina preizkušanca SENB s polmerom zarez $\rho = 1,0$ mm na mestu iniciacije razpoke (SEM, originalna povečava 70-krat)

At a lower magnification the typical chevron lines of crack propagation can be observed spreading almost from the crack root surface (**Figure 5**). The fracture surface consists mainly of ductile fracture, with the cups and cone associated with ductile cleavage. This fracture appearance is typical of the quasi-ductile fracture of high-strength steels.

4 COMPUTING THE STRESS DISTRIBUTION AT THE NOTCH TIP

The stress distribution was computed using the FEM. The typical stress distribution ahead of the stress concentrator is obtained with the opening stress normal to the notch plane plotted against the distance.

The notch radius influences the maximum stress, as we can see in **Table 3**, where the calculated stress-concentration factor is given for different notch radii. The stress-concentration factor increases with a decreasing notch radius. These values are close to Peterson's value⁵. This confirms the elastic behaviour of the selected material and the accuracy of the computation.

Table 3: Evolution of the stress-concentration factor with notch radius

Tabela 3: Faktor koncentracije napetosti v odvisnosti od ostrine zarez preizkušancev

Notch radius (mm)	0.15	0.4	0.6	0.8	1.0
Stress-concentration factor (FEM)	6.14	3.82	3.16	2.77	2.52
Stress-concentration factor (Peterson)	6.21	3.89	3.22	2.82	2.59

The elastic and elastic-plastic normal stress distribution at the notch tip decreases with the distance from the notch tip. A careful analysis has shown that this distribution can be presented using a bi-logarithmic graph⁴, and characterised by three zones: the first one very near the notch tip, where the normal stress is practically constant and/or increasing to its maximum value $\sigma_{yy,max}$; the intermediate zone between the first and third zones; and the third, which can be simulated as a pseudo-stress singularity. It is approximately described by a linear dependence (**Figure 6**). In this part the stress distribution can be represented with the following relationship:

$$\sigma_{yy} = \frac{K_{\rho}}{(2\pi r)^{\alpha}} \quad (2)$$

where K_{ρ} is the so-called *Notch Stress Intensity Factor (NSIF)* that characterises the stress gradient at the notch root in the pseudo singularity zone. This notch stress-intensity factor gives a description of the stress gradient at the notch tip and plays an important role in fractures emanating from the crack and notches. The exponent α is a parameter characterising the pseudo-stress singularity at the notch tip.

It is assumed that the fracture process needs a physical volume. This assumption is supported by the

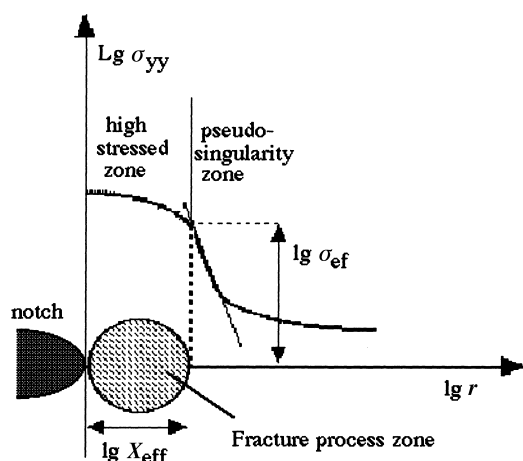


Figure 6: Schematic representation of a local stress criterion for a fracture emanating from notches⁴

Slika 6: Shematična predstavitev lokalnega napetostnega merila za zlom, ki je posledica zareznege vpliva⁴

fact that the fracture resistance is affected by the loading mode, the structure geometry and the scale effect. The value of the "hot spot stress", i.e., the maximum stress value, is unsuitable for explaining the influence of these parameters on the fracture resistance. The stress value and the stress gradient in the neighbourhood of any point in the fracture process volume are taken into account. This volume is assumed to be quasi-cylindrical by analogy with the notch plastic zone, which has a similar shape. The diameter of this cylinder is called the effective distance X_{ef} . The fracture stress can be estimated from the average value of the stress distribution along this effective distance.

It has been suggested that the effective distance corresponds to the distance from the notch tip to the boundary between zones II and III (Figure 7). The effective distance X_{ef} can be determined by making the following assumptions:

- the effective distance is greater than the plastic zone diameter;

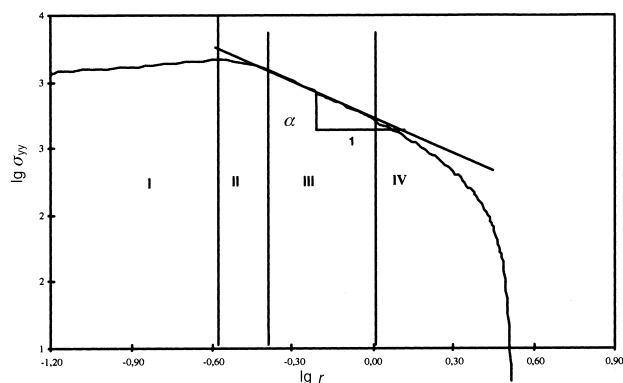


Figure 7: Stress distribution at the notch tip of a Charpy V specimen presented in a bi-logarithmic-scale graph⁴

Slika 7: Porazdelitev napetosti v vrhu zarezne preizkušanca Charpy V, predstavljena na logaritemskem diagramu⁴

- the effective distance can be defined as the diameter of the process volume, assuming that it has a cylindrical shape;
- the effective distance has to be localised into a highly stressed region where the stress gradient is not too high.

In order to determine these values exactly, the relative stress gradient χ was determined using the expression:

$$\chi = \frac{1}{\sigma_{yy}} \cdot \frac{d\sigma_{yy}}{dr} \tag{3}$$

and plotted against the distance from the notch root for each normal distribution. According to the second condition the effective distance should be localised in a region of small gradient that should be characterised by a minimum on the plot of χ against distance. This minimum corresponds to the abscissa of the upper limit of zone II and its distance from the notch root was suggested as the effective distance X_{ef} . The computed values of effective distance and effective stress obtained according to the volumetric method are listed in Table 4. The calculated effective distances X_{ef} are very high, and it seems they are not realistic for this type of material.

Table 4: Computed values of effective distance and effective stress

Tabela 4: Izračunane vrednosti efektivnih razdalj in napetosti za posamezne ostrine zazeze

ρ /mm	σ_{ef} /MPa	X_{ef} /mm
0.15	2404.0	0.11356
0.40	2264.0	0.18316
0.60	2078.0	0.28400
0.80	2009.4	0.37455
1.00	1968.0	0.40258

Generally, for the plain strain condition the plastic zone size d_y is estimated with the following equation if the fracture toughness K_{Ic} and the yield strength σ_y of the material are known⁹:

$$d_y = \frac{1}{3\pi} \cdot \left(\frac{K_{Ic}}{\sigma_y} \right)^2 \tag{4}$$

For the investigated steel, K_{Ic} is approximately 10–20 $\text{MPa}\sqrt{\text{m}}$, and the yield strength σ_y is approximately 1500–1700 MPa. From equation (4) the calculated plastic zone size d_y is then from 4 to 210 μm : almost two orders of magnitude smaller than the values for X_{ef} given in Table 4.

5 DISCUSSION

The fracture toughness has been obtained using three methods. The first method considers the notch as a crack and uses the classical linear fracture mechanics formula used for standard three-point fracture bending tests. This

method gives an apparent fracture toughness value K_c^* according to the following relationship:

$$K_c^* = \frac{P_c S_e}{BW^{3/2}} \cdot F_p(a/W) \quad (5)$$

where P_c is the critical load, S_e is the span, B is the thickness, W is the width and $F_p(a/W)$ a geometrical correction factor given in the standard ($F_p(a/W) \approx 2.66$ in our case).

The second method is Creager's method⁶. Creager considers that the stress distribution at a notch tip for a distance greater than $\rho/2$ is similar to that of a crack, and has a power dependence of 0.5. For a distance less than $\rho/2$, the stress is constant and equal to the maximum stress. The fracture toughness $K_{\rho,c}^+$ is defined as a notch stress-intensity factor with an effective stress equal to the maximum stress and an effective distance equal to $\rho/2$:

$$K_{\rho,c}^+ = \sigma_{\max,c} \sqrt{\frac{\pi \cdot \rho}{2}} \quad (6)$$

The third method is the notch fracture-mechanics method, where the real stress distribution is computed to obtain an effective stress and an effective distance, and leads to the critical notch stress-intensity factor as a fracture toughness:

$$K_{\rho,c} = \sigma_{\text{ef}} \sqrt{2\pi X_{\text{ef}}} \quad (7)$$

The critical fracture load is converted into the fracture toughness K_c^* , $K_{\rho,c}^+$ and $K_{\rho,c}$ with units MPa $\sqrt{\text{m}}$. The fact that the used notches have parallel sides with a notch angle $\Psi = 0^\circ$ leads to a power-stress distribution at the notch tip with an exponent $\alpha = 0.5$. In this particular case a comparison between different methods is possible. Then it is assumed that the evolution of the critical

notch-stress intensity factor with the notch radius obeys the following linear relationship:

$$K_{\rho,c} = A\sqrt{\rho} + K_{Ic} \quad (8)$$

On the basis of the obtained experimental results and equation (7) we can calculate $A = 51.5 \text{ MPa}$ and $K_{Ic} = 56.5 \text{ MPa}\sqrt{\text{m}}$ (Figure 8). The values of K_{Ic} obtained with extrapolation ($\rho = 0$) are much higher than those obtained on the precracked cylindrical specimens ($K_{Ic} \approx 8\text{--}14 \text{ MPa}\sqrt{\text{m}}$)⁷⁻⁸, as well as the values found in the literature⁹ for this type of material ($K_{Ic} \approx 10\text{--}20 \text{ MPa}\sqrt{\text{m}}$). The main reason is probably the too large values of the effective distances X_{ef} obtained from the FEM calculations. Therefore, additional FEM calculations, as well as microstructural investigations of the plastic zone and experiments with pre-cracked SENB specimens have to be performed in the future.

We can also see (Figure 8) that the fracture toughness K_c^* calculated according to Creager is much lower and closer to the experimental values obtained with the pre-cracked cylindrical specimens.

The values for the apparent fracture toughness K_c^* are also unrealistically high and relatively close to the critical notch stress-intensity factor $K_{\rho,c}$. The reason is that the geometrical correction factor $F_p(a/W)$ is not constant and changes drastically with the increased notch-root sharpness.

6 CONCLUSIONS

For hard and brittle steels, where fracture-toughness tests with pre-cracked specimens are difficult to perform, it is possible to estimate the fracture toughness with notched non-pre-cracked specimens. It is a relatively fast, cheap and easy method. However, in most cases it seems that a simple linear approximation from $\rho \gg 0$ (notch stress-intensity factor $K_{\rho,c}$) to $\rho \approx 0$ (fracture toughness K_{Ic}) leads to a rough estimation, and in this way the obtained values for K_{Ic} have to be considered very carefully.

ACKNOWLEDGEMENT

The authors are grateful to the Slovenian Ministry of Education, Science and Sport and to the France R&D authorities for their financial support in the frame of the bilateral Slovenia-France programme Proteus.

7 REFERENCES

- O. Akkouri, M. Louah, A. Kifani, G. Gilgert, G. Pluvinae: The effect of notch radius on fracture toughness J_{Ic} . Eng. Fract. Mech., 65(2000), 491–505
- L. Toth, Proceedings of 1-st ILSSCRSS Meeting, Miskolc, Hungary, 1995
- M. Aberkane, G. Lenkey, G. Pluvinae: Notch effects and fracture toughness of cast steels used for nuclear waste containers, 16-th

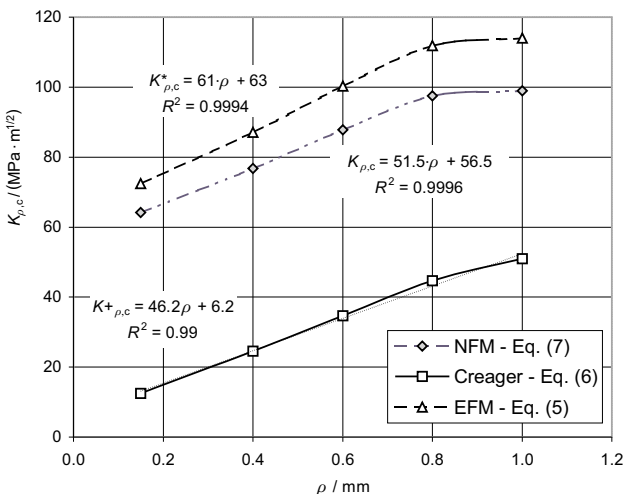


Figure 8: Evolution of the apparent fracture-toughness value K_c^* , the fracture toughness $K_{\rho,c}^+$ according to Creager $K_{\rho,c}^+$ and the critical notch stress-intensity factor $K_{\rho,c}$ with a dependence on the square root of the notch radius

Slika 8: Navidezni faktor intenzitete napetosti v zarezih K_c^* , $K_{\rho,c}^+$ izračunan po Creagerju in kritični faktor intenzitete napetosti v zarezih $K_{\rho,c}$ v odvisnosti od kvadratnega korena polmera zareze

International Conference on Structural Mechanics in Reactor Technology, Washington DC, August 12–17, 2001, CD, 1–8

- ⁴G. Pluinage, M. Gjonaj: Notch effects in fatigue and fracture, *Nato Sciences Series*, 11 (**2001**), 1–22
- ⁵R. E. Peterson: *Stress concentration Factors*, John Wiley and Son, New York, 2, (**1974**), 59
- ⁶M. Creager, C. Paris: Elastic field equations for blunt cracks with reference to stress corrosion cracking, *International Journal of Fracture*, (**1967**)3, 247–252
- ⁷V. Leskovšek, B. Šuštaršič, T. V. Pirtovšek, F. Grešovnik, G. Jutriša: Fracture toughness K_{Ic} : a selection criterion for the heat treatment of high-speed steels, *Materials and technology*, 36(**2002**)6, 337–341
- ⁸V. Leskovšek, B. Ule, B. Lišičić: Relations between fracture toughness, hardness and microstructure of vacuum heat-treated high-speed steel, *Journal of Materials Processing Technology*, 127(**2002**)3, 298–308
- ⁹S. A. Horton: Ph.D. Thesis, University of Aston, Birmingham, UK, 1980